New Phytologist

The *Aquilegia JAGGED* homolog promotes proliferation of adaxial cell types in both leaves and stems

Ya Min and Elena M. Kramer

Department of Organismic and Evolutionary Biology, Harvard University, 16 Divinity Ave., Cambridge, MA 02138, USA

Author for correspondence:
Elena M. Kramer
Tel: +1 617 496-3460
Email: ekramer@oeb.harvard.edu

Received: *5 August 2016*
Accepted: *14 September 2016*

New Phytologist (2017) **216:** 536–548
doi: 10.1111/nph.14282

Key words: *Aquilegia*, cell proliferation, flower morphogenesis, *JAGGED*, leaf morphogenesis, polarity, primordium initiation.

Summary

- In order to explore the functional conservation of *JAGGED*, a key gene involved in the sculpting of lateral organs in several model species, we identified its ortholog *AqJAG* in the lower eudicot species *Aquilegia coerulea*.
- We analyzed the expression patterns of *AqJAG* in various tissues and developmental stages, and used RNAi-based methods to generate knockdown phenotypes of *AqJAG*.
- *AqJAG* was strongly expressed in shoot apices, floral meristems, lateral root primordia and all lateral organ primordia. Silencing of *AqJAG* revealed a wide range of defects in the developing stems, leaves and flowers; strongest phenotypes include severe reduction of leaflet laminae due to a decrease in cell size and number, change of adaxial cell identity, outgrowth of laminar-like tissue on the inflorescence stem, and early arrest of floral meristems and floral organ primordia.
- Our results indicate that *AqJAG* plays a critical role in controlling primordia initiation and distal growth of floral organs, and laminar development of leaflets. Most strikingly, we demonstrated that *AqJAG* disproportionally controls the behavior of cells with adaxial identity in vegetative tissues, providing evidence of how cell proliferation is controlled in an identity-specific manner.

Introduction

The seemingly infinite variety of forms of leaves and floral organs is achieved by a complex interplay of cell proliferation and expansion. These processes are controlled by a number of fine-tuned programs that are executed with temporal and spatial precision, making decisions about the rate, orientation and duration of cell division and differentiation. Throughout the process of morphogenesis, many of these programs are regulated based on the adaxial–abaxial axis of the lateral organ. This axis is established soon after the organ primordium becomes distinguishable from the meristem, as cells adjacent to or away from the meristem acquire adaxial and abaxial identity, respectively. The genetic programs determining these polarities are strikingly conserved across plant taxa, in which genes including the class III homeodomain-leucine zipper transcription factors control adaxial identity, whereas genes such as the KANADIs (KAN) and *ETTIN/ARF3* control abaxial identity (Emery *et al.*, 2003; Harrison *et al.*, 2005; Pekker *et al.*, 2005).

It is widely accepted that laminar expansion in lateral organs is induced by the boundary where the adaxial and abaxial domains meet (Waites & Hudson, 1995). Therefore, modification of this boundary or differential development of adaxial and abaxial tissues is one mechanism to generate diversity in organ form. For instance, modifications of organ polarity have been implicated in a range of morphologies, from the pitcher leaves of *Sarracenia purpurea* (Fukushima *et al.*, 2015) to the narrow filaments and broad anthers of rice stamens (Toriba *et al.*, 2010). Nonetheless, even for a simple flat leaf, the developmental patterns of the adaxial and abaxial domains are by no means identical: spongy mesophyll cells stop dividing before the overlying palisade mesophyll cells, and are then separated during the active proliferation of the latter, resulting in loosely packed spongy cells with air space on the abaxial side, and densely packed palisade cells on the adaxial side (Dale, 1988).

Although the precise mechanism of how cell proliferation and expansion are controlled in response to abaxial vs adaxial identities remains elusive, research on model species such as Arabidopsis (*Arabidopsis thaliana*) and rice (*Oryza sativa*) have discovered a number of genes that generally promote or restrict organ growth, providing a useful starting point to explore this question. For example, members of the *YABBY* and *WUSCHEL-RELATED HOMEOBOX* family are downstream of polarity determinants and are thought to integrate polarity signals to promote lamina outgrowth (Siegfried *et al.*, 1999; Eshed *et al.*, 2004; Vandenbussche *et al.*, 2009; Sarojam *et al.*, 2010; Nakata *et al.*, 2012). Genes such as the *BLADE ON PETIOLE* (*BOP*) family have been found to shape the basal portion of lateral organs (e.g. leaf petiole), preventing outgrowth of laminae by interacting with polarity genes (Ha *et al.*, 2007; Jun *et al.*, 2010). As a counterpart to the *BOP*s, *JAGGED* (*JAG*) promotes growth of the distal portion of the lateral organ, maintaining active cell proliferation and expansion until the organ reaches the final size (Dinneny *et al.*, 2004; Ohno *et al.*, 2004).

In this study, we identify the *JAG* homolog (*AqJAG*) in the lower eudicot species *Aquilegia coerulea* and investigate its functions during *A. coerulea* morphogenesis. *JAG* encodes a

C2H2-type zinc-finger transcriptional factor that is broadly expressed in all lateral organs in Arabidopsis. Its null mutant displays reduced development in the distal regions of lateral organs, whereas overexpression of *JAG* leads to ectopic blade tissue growth and formation of bracts (Dinneny *et al.*, 2004; Ohno *et al.*, 2004). *NUBBIN* (*NUB*), a close paralog of *JAG,* has been been identified only in Arabidopsis (Dinneny *et al.*, 2006), and, unlike *JAG*, is expressed strictly in the adaxial domain of lateral organs. Single *nub* mutants display no apparent defect, whereas *jag nub* double mutants show a more severe version of the *jag* single mutant, and thus *JAG* and *NUB* are thought to work redundantly to promote proliferation in the distal regions of lateral organs. Complete loss-of-function of mutants in the *JAG* homologs *LYRATE* (*LYR*) and *OPEN BEAK* (*OPB*) also have been characterized in tomato (*Solanum lycopersicum*) and rice, respectively (David-Schwartz *et al.*, 2009; Horigome *et al.*, 2009). These mutants are similar to *jag nub* in that they show impaired laminar growth, but also differ in several aspects, including the formation of fewer lateral leaflets in *lyr* compound leaves, and reduced expression levels of B class floral identity genes in *opb* flowers.

Our particular interest in *Aquilegia JAG* homolog function stems from our ongoing analysis of the developmental programs controlling several novel floral organ types. *Aquilegia* flowers possess elongated nectar spurs on their petals, which previous studies have shown are best understood as dramatic examples of laminar curvature (Yant *et al.*, 2015). In addition, *Aquilegia* produces a fifth organ type, the staminodium, which appears to be derived from sterilized, laterally expanded stamens (Sharma & Kramer, 2013b). Although these features are relatively recently evolved, analysis of gene function in *Aquilegia* can also shed light on broader patterns of functional evolution and help bridge the deep phylogenetic divergence between core eudicot and monocot models (Kramer & Hodges, 2010). We used virus-induced gene silencing (VIGS) to generate knockdown phenotypes of *AqJAG*, demonstrating that it plays a critical role in *Aquilegia coerulea* flower and leaf development. Most strikingly, we demonstrate that *AqJAG* disproportionally affects the behavior of cells with adaxial identity in vegetative tissues. Our results show that *AqJAG* promotes both cell proliferation and the ability of cells to properly respond to their identity, which provides insight into the mechanisms by which proliferation is controlled differentially in the context of organ polarity.

Materials and Methods

Identification of the candidate gene

The complete DNA sequence of *AqJAG* was obtained via BLAST (Basic Local Alignment Search Tool; Altschul *et al.*, 1990) using the cDNA sequence of *JAGGED* (*JAG*) from Arabidopsis against the *Aquilegia coerulea* (James) genome on PHYTOZOME (http://www.phytozome.net/). A reverse BLAST search of the translated amino acid sequence of the putative *AqJAG* against an Arabidopsis protein database (www.arabidopsis.com) also identified JAG with the highest score. To confirm the orthology of *AqJAG* (*Aquilegia* genome v3.1 locus Aqcoe3G037600, GenBank accession KX879697), a 56-locus alignment containing putative *JAG* homologs from a variety of land plant taxa was constructed via BLAST searches in GenBank, PHYTOZOME and the DFCI Plant Gene Index (http://compbio.dfci.harvard.edu/cgi-bin/tgi/plant.html). Information regarding 14 other related zinc-finger proteins in Arabidopsis was obtained from previous family analyses (Englbrecht *et al.*, 2004; Ciftci-Yilmaz & Mittler, 2008). All amino acid sequences were aligned using CLUSTALW (Larkin *et al.*, 2007) and then adjusted by hand using MACVECTOR (Cary, NC, USA). The phylogenetic analysis was performed using the CIPRES web portal (http://www.phylo.org/portal2/login!input.action). A maximum-likelihood tree was constructed using randomized axelerated maximum likelihood (RAxML; Stamatakis *et al.*, 2008) implemented with the default Jones–Taylor–Thorton (JTT; Jones *et al.*, 1992) model of amino acid substitution. The resultant tree was displayed by software program FIGTREE v.1.3.1 (http://tree.bio.ed.ac.uk/software/figtree/).

In situ hybridization

A 465-bp DNA fragment in a nonconserved region of *AqJAG* was amplified (forward primer: 5′-TCTACACACCGTCATCTTCTCG-3′; reverse primer: 5′-TGTCAGTTGTTTGGTTTCTATCTG-3′) and cloned into the pCR™4-TOPO® vector. Both sense and anti-sense probes were alkaline-hydrolyzed at 60°C for 41 min to an average length of 150 bp. All *in situ* hybridization steps were performed as described by Kramer (2005). Results were visualized in the Harvard Center for Biological Imaging on a Zeiss AxioScan microscope using trans-illumination with white light.

Virus-induced gene silencing

Virus-induced gene silencing (VIGS) was performed according to protocols described previously (Gould & Kramer, 2007; Sharma & Kramer, 2013a). The TRV2 vector containing a fragment of *A. coerulea ANTHOCYCANIDIN SYNTHASE* (*AqANS*-TRV2) as a marker of the target gene silencing has been previously prepared and described (Gould & Kramer, 2007). The same 465-bp *AqJAG* fragment amplified for *in situ* hybridization was cloned into the *AqANS*-TRV2 plasmid to generate the *AqJAG-AqANS*-TRV2 construct, which was subsequently transformed into GV3101 electrocompetent *Agrobacterium* cells. Three hundred plants were infiltrated with *AqJAG-AqANS*-TRV2 construct and 100 plants were treated with *AqANS*-TRV2 construct as controls. Plants showing knockdown phenotypes were documented and photographed using a Canon X type digital SLR camera (Canon, Melville, NY, USA).

Scanning electron microscopy and histology

Organs of interest were fixed in FAA (50% ethanol, 4% formalin and 5% glacial acetic acid) and stored at 4°C. For scanning electron microscopy (SEM), samples were dehydrated through a graded ethanol series to 100% EtOH at 4°C and critical point-dried before imaging. Materials were imaged using a JEOL

JSM-6010 LC Scanning Electron Microscope. Samples for histology were dehydrated through the same graded ethanol series, stored in 100% Citrasolv, and embedded in Paraplast Plus (Oxford Labware, St Louis, MO, USA). Tissues were sectioned to 8 μm using a rotary microtome and stained with 0.01% Safranin O and 50% Fast Green according to the protocol described in Ruzin (1999). The wild-type (WT) and *AqJAG*-silenced stems were collected when the terminal flowers were opened, and sections were processed in parallel. Slides were photo-documented in the Harvard Center for Biological Imaging on a Zeiss AxioScan microscope using trans-illumination with white light.

Quantitative real-time polymerase chain reaction

Total RNA was extracted from flower buds from *AqJAG-AqANS*-TRV2- and *AqANS*-TRV2-treated plants using PureLink Plant RNA Reagent (Invitrogen), and treated with Turbo DNAse (Ambion). cDNA was synthesized from 1 μg of RNA using Superscript II reverse transcriptase (Invitrogen) and oligo (dT) primers. The resulting cDNA was diluted 1 : 10 as template. Brilliant II SYBR Green QPCR Master Mix, Low ROX (Stratagene, Cedar Creek, TX, USA/La Jolla, CA, USA), was used to carry out the quantitative real-time polymerase chain reactions (qRT-PCR) in the Stratagene Mx3005P QPCR System. QRT primers for *AqJAG* were designed to span the intron positions (forward primer: 5′-GGTGGAAAAGATGAGTGTGGG-3′; reverse primer: 5′-AAATGAGGACCCCCTTGTGC-3′). *AqIPP2* (*ISO PENTYL PYROPHOSPHATE:DIMETHYLALLYL PYROPHOS PHATE ISOMERASE2*) was used for normalization as it has been shown previously to have little quantitative transcriptional variation across tissues and developmental time points (Sharma *et al.*, 2011). Primer efficiencies were evaluated before the expression analysis using six dilution series. Eight biological replicates for both control and *AqJAG* VIGS group were examined. Expression for each biological sample was assayed from three replicates per reaction plate. The variability resulting from technical replicates was negligible compared with the variability from biological replicates, so only biological variability is presented here. Relative gene expression levels were calculated using the $2^{-\Delta\Delta CT}$ method described in Livak & Schmittgen (2001), and formulas were adjusted with the obtained primer efficiencies for both *AqJAG* and *AqIPP2*. An unpaired Student's *t*-test was used to determine the statistical significance of differences between experimental and control values.

Results

Identification of *AqJAG*

The putative *JAG* homolog in *A. coerulea* genome is a 2690-bp-long single copy gene that is predicted to encode 423 amino acid residues. Consistent with the structure of JAG in Arabidopsis, AqJAG possesses characteristic features of a C2H2 type zinc-finger protein, specifically a single zinc-finger domain, as well as a conserved QALGGH sequence, a proline-rich motif positioned towards the C-terminal and an ERF-associated amphiphilic repression (EAR) motif (Supporting Information Fig. S1). In order to determine the correct orthology of *AqJAG*, we constructed a maximum-likelihood tree using the amino acid sequences from 42 putative JAG homologs from various land plant taxa, as well as 14 C2H2 zinc-finger proteins with one or two zinc-finger domain(s) from Arabidopsis (Fig. S2). The phylogeny was rooted by using sequences with two zinc-finger domains as an outgroup. This produced a tree in which all putative JAG homologs, including AqJAG, cluster into a large clade with strong bootstrap support (95%), whereas the other seven proteins with a single zinc-finger domain from Arabidopsis resolved into a separate clade. Within the JAG clade, many branches did not show strong support due to the combined facts that the conserved domains are very highly conserved, and therefore have little phylogenetic information, whereas other regions of the genes show relatively low conservation and are therefore too variable to resolve deeper nodes. Nevertheless, although the phylogenetic position of *AqJAG* within the *JAG* homolog clade cannot be fully resolved with high confidence, our analysis has sufficient power to show that we have identified the correct *JAG* ortholog in *A. coerulea*.

AqJAG is strongly expressed in meristems, lateral organ primordia and regions undergoing rapid growth

A detailed picture of the specific spatial and temporal patterns of *AqJAG* expression in different tissues and developmental stages in *A. coerulea* was obtained by *in situ* hybridization (developmental stages of *Aquilegia* flowers in Table S1). Strong signal of *AqJAG* was detected in shoot apical meristems (Fig. 1a), leaf primordia (Fig. 1a), lateral root primordia (Fig. 1b), floral meristems (Fig. 1d–i) and all initiating floral organ primordia (Fig. 1e–i). During stage 7 of flower development, when the stamens became stalked at the base and the anthers started to differentiate, hybridization signal in stamens declined in the filament and became concentrated in the anthers (Fig. 1h). Meanwhile, the staminodia became distinguishable from stamens, with higher concentration of *AqJAG* expression in their distal tips (Fig. 1g,h). Signal disappeared when staminodia began to flatten in stage 9 (Fig. 1i). *AqJAG* was highly expressed in the distal region of the carpels from their inception, but moderate expression could also be seen throughout the carpels during all developmental stages (Fig. 1g,h). Subsequently, signals were detected in the initiating ovules in the carpels (Fig. 1i). When the flower transitions into stage 10 and onward, petal primordia continue differentiating and initiate petal spurs, and strong expression can be detected throughout the petals (Fig. 1i; later stage data not shown). No expression was observed with sense probe (Fig. 1c).

VIGS silencing of *AqJAG*

In order to knock-down the expression of *AqJAG*, we cloned a 465-bp fragment from a nonconserved region of *AqJAG* together with a fragment of gene *AqANS* into the multiple cloning site of TRV2 vector. *AqANS* has been used previously as an indicator of gene silencing from VIGS in *A. coerulea* flowers, and it has been demonstrated that plants infiltrated with *AqANS*-TRV2 show no

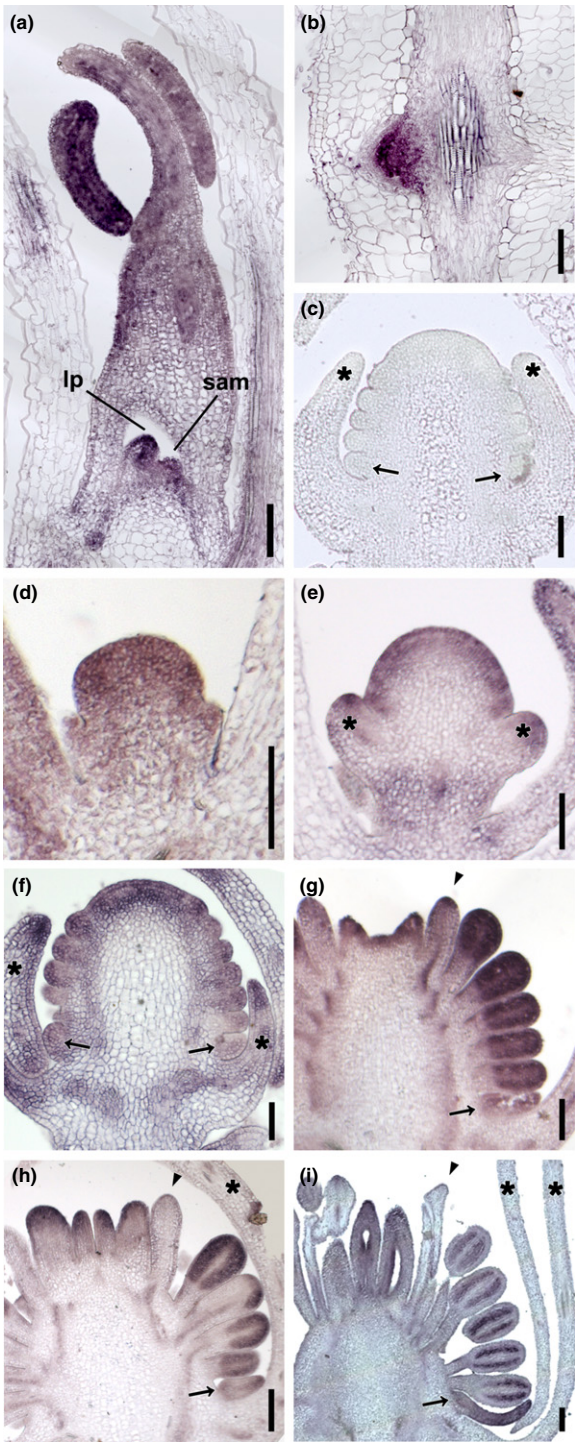

Fig. 1 Expression patterns of *AqJAG* in *Aquilegia coerulea* (a) vegetative meristems and leaf primordia, (b) lateral root primordia, and (d–i) early stages of flower development. (c) Hybridization with sense probe. (d) Stage 2 floral meristem. (e) Stage 3 floral meristem; only sepal primordia initiated. (f) Stage 6 floral meristem; all organ primordia except carpels initiated. (g) Stage 7 young flower bud with carpels just initiated. (h) Stage 9 young flower bud. (i) Stage 10 flower bud with flattened staminodia. lp, leaf primordia; sam, shoot apical meristem; asterisk, sepal primordia; arrow, petal primordia; arrowhead, staminodium. Bars, 100 μm.

morphological change from the WT aside from a loss of anthocyanin in vegetative and floral tissues (Sharma & Kramer, 2013a). The *AqANS*-TRV2 construct was used as VIGS control.

In order to assess the downregulation of *AqJAG* in the VIGS-treated plants, we subsequently performed qRT-PCR (Fig. S3). We collected young axillary buds from inflorescences showing strongly silenced phenotypes (see below). After normalizing the expression levels with the housekeeping gene *AqIPP2*, the relative expression levels of *AqJAG* were significantly lower in the *AqJAG* VIGS samples compared with those of control plants (Student's *t*-test, $P < 0.005$), indicating that the observed phenotypes were indeed due to the silencing of *AqJAG* expression.

AqJAG-silencing results in severe lamina reduction and concave curvature in leaves

A typical WT *A. coerulea* rosette leaf consists of three parts: a large pair of stipules at the leaf base, a long petiole and a ternate compound lamina in which each leaflet is usually deeply lobed or further segmented (Fig. 2a; Kramer & Hodges, 2010; Pabón-Mora *et al.*, 2013). The petiolules are not as elongated as the petioles and higher order petiolules with leaflets are usually only observed in leaves produced after vernalization (Fig. 2a).

Among our *AqJAG*-treated plants, there was no change in the overall number of leaflets or segments per leaflet, but *c.* 31% exhibited a decrease in leaflet area, usually accompanied by reduction in petiolule length (Fig. 2b–h). The degree of laminar reduction varied greatly, reflecting the variation typically seen with VIGS-based silencing. Some leaflets only had small patches of effected lamina, whereas the remaining parts of the leaflet underwent normal cell proliferation and expansion, leading to asymmetric morphologies of the leaflets (e.g. leaflet segments in Fig. 2b–d). Normal leaf margin formation was often disrupted in these leaflets due to the impaired coordination of growth between the silenced and unsilenced regions (Fig. 2b–d). A number of plants also exhibited severe reduction in the entire lamina, resulting in significantly smaller leaflets (Fig. 2b–h). In the strongest silencing phenotypes, the lamina was so reduced that it became almost indistinguishable from the petiolule, appearing as an extremely stunted structure (Fig. 2d,h).

In addition, when looking at the leaves from the adaxial side, all leaflets experiencing laminar reduction were concave, at least in part (Fig. 2b–g), with an apparent association between the degree of growth repression and the severity of curvature (Fig. 2d–h). In some case, the entire lamina was concave, forming a bowl-like structure (Fig. 2c–g).

AqJAG-silenced leaves show a decrease in cell number and a change in adaxial cell identity

We analyzed the strongest phenotype of *AqJAG*-silenced leaves using SEM, and determined that the stunted structures are, in fact, differentiated ternate leaflet primordia in which the leaflet laminae failed to develop and expand (Fig. 3a). Disruption in the

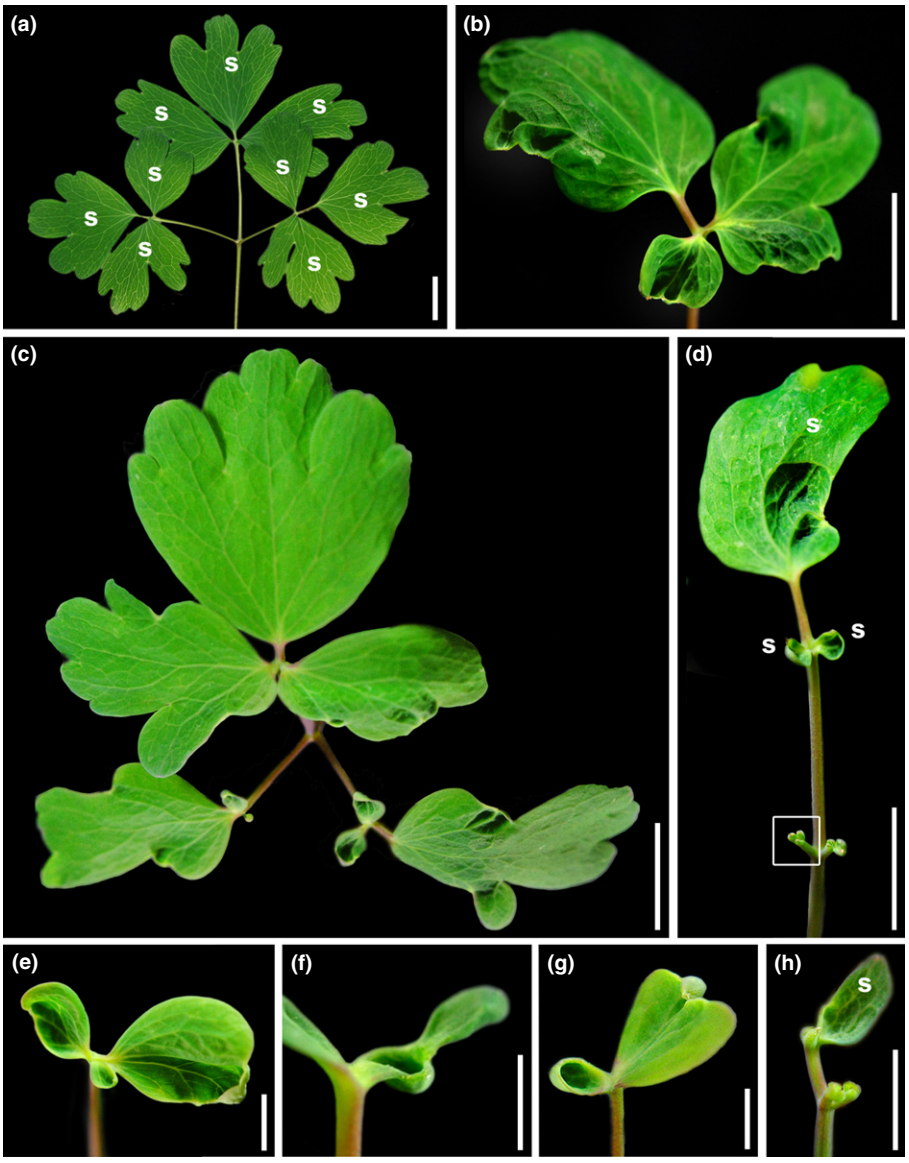

Fig. 2 Phenotypes of *AqJAG* VIGS leaves of *Aquilegia coerulea*. (a) A wild-type (WT) rosette leaf with three leaflets. Each leaflet is further divided into three segments with different degrees of lobing. (b–h) *AqJAG-AqANS*-TRV2-treated leaves showing a wide range of silencing phenotypes. (b) Leaflet with patches of affected laminae that are concave. (c) An *AqJAG*-silenced leaf with one unaffected central leaflet and two partially silenced lateral leaflets that display varying degrees of laminar reduction and curvature. (d) An *AqJAG*-silenced leaf showing three different degrees of silencing. Terminal leaflet is moderately silenced whereas lateral leaflets are strongly silenced. Box indicates the leaflet used for scanning electron microscopy (SEM) shown in Fig. 3(a). (e–g) Close up views of *AqJAG*-silenced leaflets showing various degrees of concave curvature. (h) Close-up of an *AqJAG*-silenced leaf with only one segment of the central leaflet showing any expanded laminar area, whereas all other segments and leaflets are highly reduced with no lamina. s, segments of leaflets. Bars: (a–d) 1 cm; (e–h) 5 mm.

development of the laminar margin and extreme curvature of the laminae were both prominent. For leaves exhibiting this severe laminar reduction, no WT marginal cells, trichomes, or vascular strands were observed.

Furthermore, we compared the epidermal cell morphologies between WT/control and *AqJAG* VIGS-treated leaves. No difference in abaxial cell morphology was observed; the abaxial surface in all analyzed leaves from all treatment groups displayed irregular convex cells with stomata scattered across the whole surface (Fig. 3b,d). On the adaxial surface of *AqJAG*-silenced leaves, however, the cobblestone-shaped epidermal cells of WT leaves (Fig. 3c) were replaced entirely by small conical cells (Fig. 3e). These cells do not especially resemble the cell types found in other lateral organs, including floral organs. Given that no change in cell size or shape was found on the abaxial surface, we can infer that laminar reduction is associated primarily with a decrease in cell numbers in that domain. In the adaxial domain, the conical cells in *AqJAG*-silenced leaves are significantly smaller than the WT epidermal cells (up to 80% smaller), but this size difference is not entirely sufficient to explain the degree of lamina reduction, which can be as great as 97%. Based on these observations, we conclude that the reduction in laminar size in *AqJAG*-silenced leaves not only involves reduction in cell number in both the adaxial and abaxial domains, but also includes changes in cell size in the adaxial domain, apparently due to improper differentiation of cell identity.

AqJAG-silenced inflorescences display a number of novel phenotypes

Upon transition to the reproductive phase, *Aquilegia* flowers usually exhibit strong apical dominance and only a primary inflorescence will develop. Among all the *AqJAG-AqANS*-TRV2-treated plants, 43.2% showed more than one inflorescence, whereas only 8% of the VIGS control plants had secondary inflorescences (Fig. 4c), a significant difference (Pearson's χ^2 test, $P < 0.0001$). Moreover, the first internodes of the WT inflorescence axes of *Aquilegia* often extend to the same level as the rosette leaves,

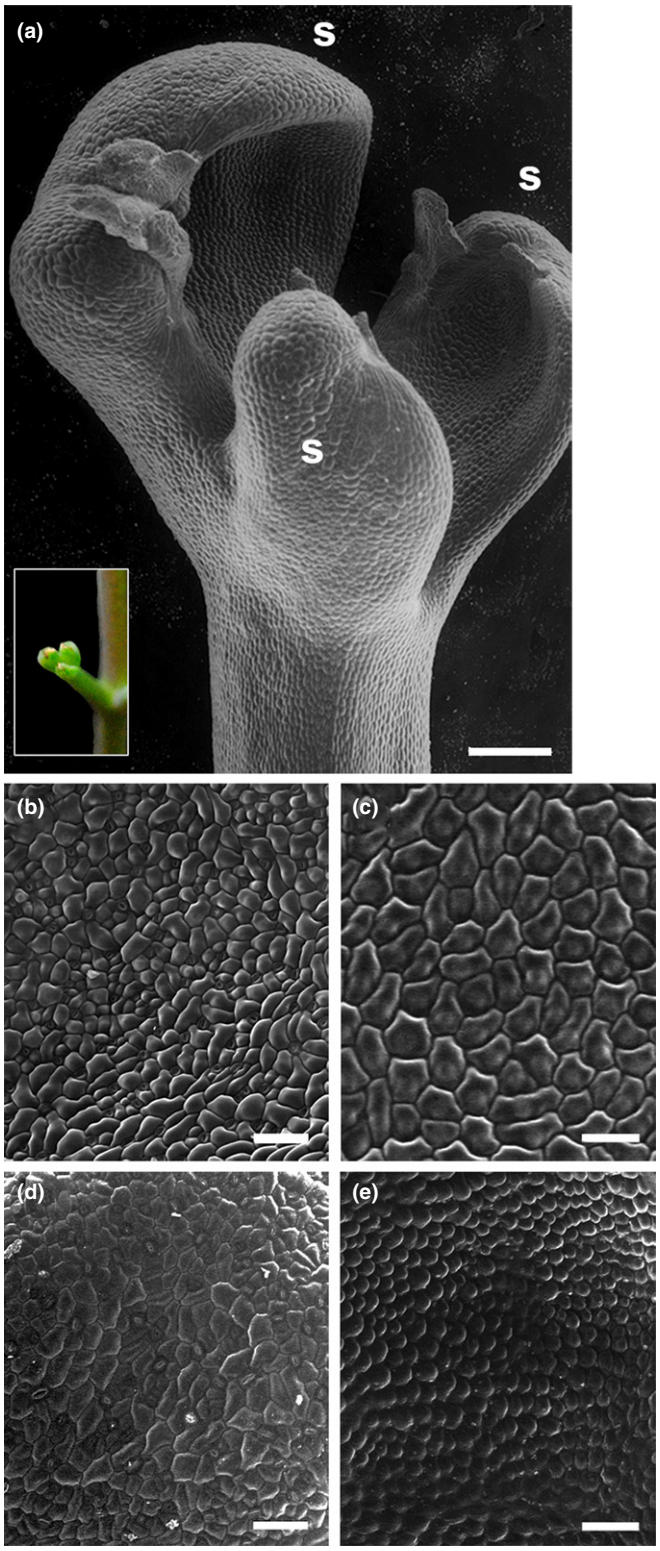

Fig. 3 Scanning electron microscopy of wild-type (WT) *Aquilegia coerulea* and *AqJAG*-silenced leaves. (a) Close-up of leaflet with the most severe silencing phenotype (inset shows lateral leaflet before fixation, also boxed in Fig. 2d). (b, c) Cells on the (b) abaxial and (c) adaxial surface of WT leaves. (d, e) Cells on the (d) abaxial and (e) adaxial surface of *AqJAG*-silenced leaves. s, segments of leaflets. Bars: (a) 200 μm; (b, d) 100 μm; (c, e) 50 μm.

meaning that flowers always bloom above the rosette leaves (Fig. 4b). However, flowers from *AqJAG* VIGS plants were often observed opening below or at the level of rosette leaves (Fig. 4c). We thus measured the length of the first internode of the inflorescences in all of the VIGS plants after the terminal flowers had opened, which revealed a significant decrease in internode length among the *AqJAG* VIGS plants (Fig. 4a).

In addition to these shortened inflorescences, we observed peculiar outgrowths on the inflorescence stem in *c.* 9% of *AqJAG* VIGS plants (Fig. 4d–f). The outgrowths resemble thin laminae with little pigmentation. In most cases, the outgrowth occurred along just one side of the stem (Fig. 4e,f), but rarely there were growths on both sides (Fig. 4d). These outgrowths were observed only on the first internodes of secondary inflorescence axes.

In order to further characterize the structural changes that led to the lamina-like outgrowths, we investigated the stem anatomy using histology. The WT inflorescence of *A. coerulea* possesses the features of a typical dicot stem lacking secondary growth (Fig. 5a): moving from the center to the outermost layer, it consists of central pith, a single ring of collateral vascular bundles, collenchyma cells for mechanical support, and epidermis. Each vascular bundle contains a pole of heavily lignified xylem oriented towards the pith and a pole of phloem positioned towards the epidermis (Fig. 5b,c).

Cross-sections of the *AqJAG*-silenced inflorescence stems all exhibited a reduced amount of collenchyma cells and a clear decrease in the amount of differentiated xylem (Fig. 5d–f). Further, the existing xylem was much less lignified compared with xylem of WT (Fig. 5c vs 5f). Most strikingly, we observed distinct differences in the morphology of vascular bundles in the region adjacent to the outgrowth as compared to within the outgrowth itself (Fig. 5e,g). Near the site of the outgrowth, the vascular bundles were clustered with no normal pattern and appeared largely to lack xylem (Fig. 5d,g). By contrast, the vascular bundles present in the outgrowths possessed well-developed xylem, but their arrangement more closely resembles that seen in a leaf (Fig. 5g).

AqJAG is essential for floral organ primordium initiation and expansion

A WT *A. coerulea* flower possesses five petaloid sepals in the outer most whorl, a whorl of five petals with pronounced nectar spurs, five to ten whorls of stamens, a whorl of ten staminodia, and five carpels in the inner most whorl (Fig. 6a–d). The petal spurs elongate very rapidly during stage 11 and reach a final length of 4–5 cm (Fig. 6a–c).

About 40% of *AqJAG* VIGS-treated plants displayed significant floral defects, which fall into four categories: defects in the distal growth of lateral organs, including jagged petal blades (Fig. 6e), jagged sepal margins (Fig. 6f), abolished and/or underdeveloped anthers (Fig. 6k–m), and petal spurs with reductions in length and width (Fig. 6f,g,l,n); mosaic organs, for which the most commonly observed were petal–sepal (Fig. 6h) or petal–stamen chimeras (Fig. 6i); missing floral organs, (Fig. 6j–n), for which missing carpels (Fig. 6k–o), staminodia (Fig. 6k–o), and

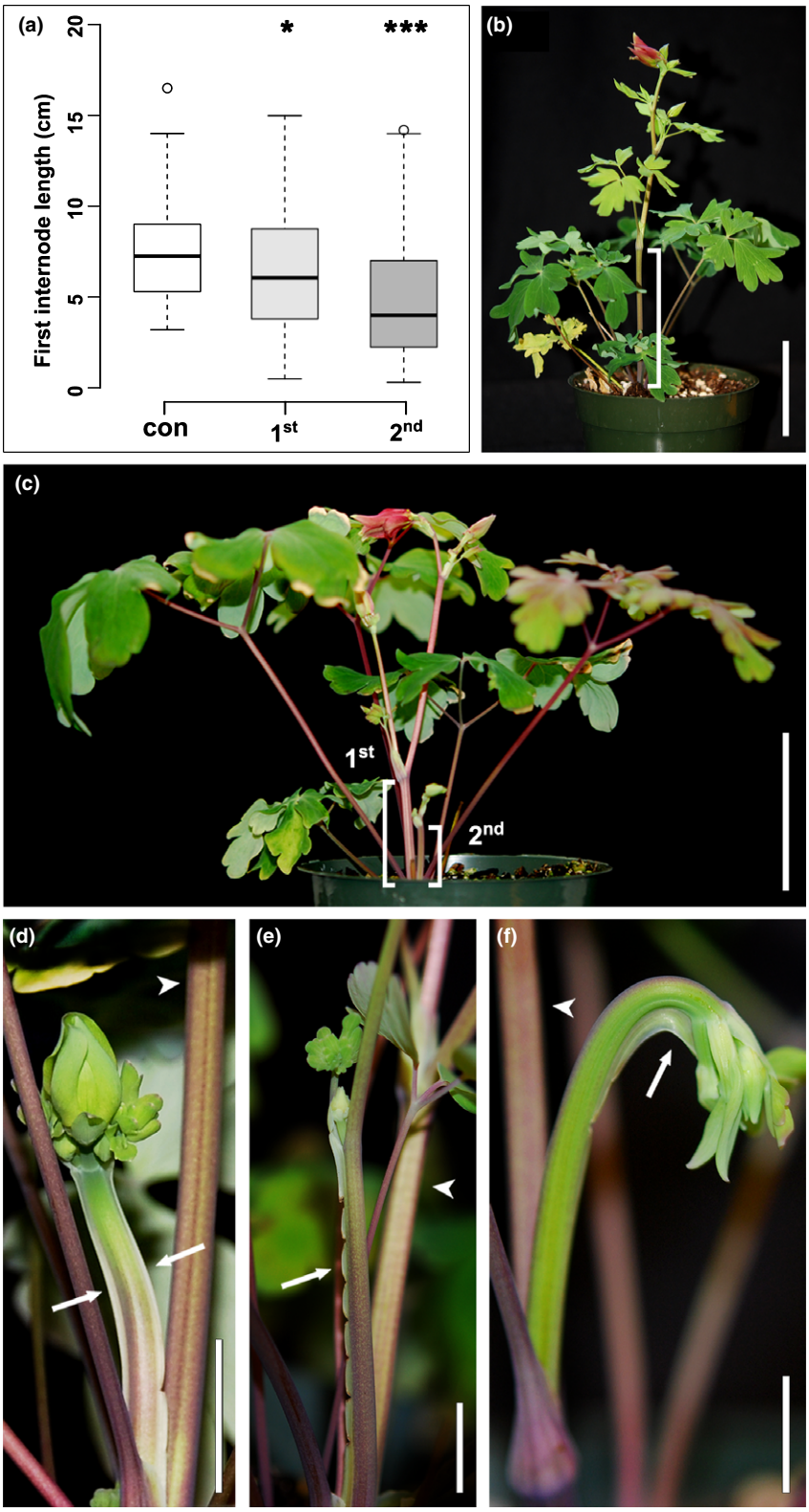

Fig. 4 *AqJAG-AqANS*-TRV2-treated *Aquilegia coerulea* plants shows a significant decrease in the length of the first inflorescence internode and peculiar outgrowths on the stem. (a) First internode lengths were measured from the primary inflorescence of all virus-induced gene silencing (VIGS) control plants (con), and the primary inflorescence (1st) and secondary inflorescence (2nd) of all *AqJAG-AqANS*-TRV2-treated plants. When there were multiple secondary inflorescences on an *AqJAG*-silenced plant, the average of the first internode lengths of all secondary inflorescences was taken. Error bars indicate ± SE and asterisks indicate the significance levels of Student's *t*-test with the control group: *, $P < 0.05$; ***, $P < 0.0005$. (b) A VIGS control plant. (c) An *AqJAG* VIGS plant showing reduced internode lengths and secondary inflorescence. (d) An *AqJAG* VIGS inflorescence with two regions of stem exhibiting outgrowth. (e) Outgrowth on the stem sometimes was torn apart into segments due to the elongation of the internode. (f) Inflorescence was bent downwards due to the outgrowth on the stem. Brackets, first internode of inflorescences; arrows, outgrowths; arrowheads, adjacent inflorescence stems without outgrowths. Bars: (b, c) 5 cm; (d–f) 1 cm.

stamens (Fig. 6k–o) were observed more often than missing petals (Fig. 6j,n,o) and sepals (Fig. 6n); a small number of 'flowers' failed to develop any floral organs, usually resulting in a small bulge of tissues with undefined identity (Fig. 6p,q). We considered this to be the most severe silencing phenotype. We further analyzed a number of flowers with missing reproductive organs using SEM to investigate whether this phenotype was resulted from initiated but underdeveloped primordia, but no initiated primordium was found in any sample and the center meristem was always completely consumed (e.g. Fig. 6m).

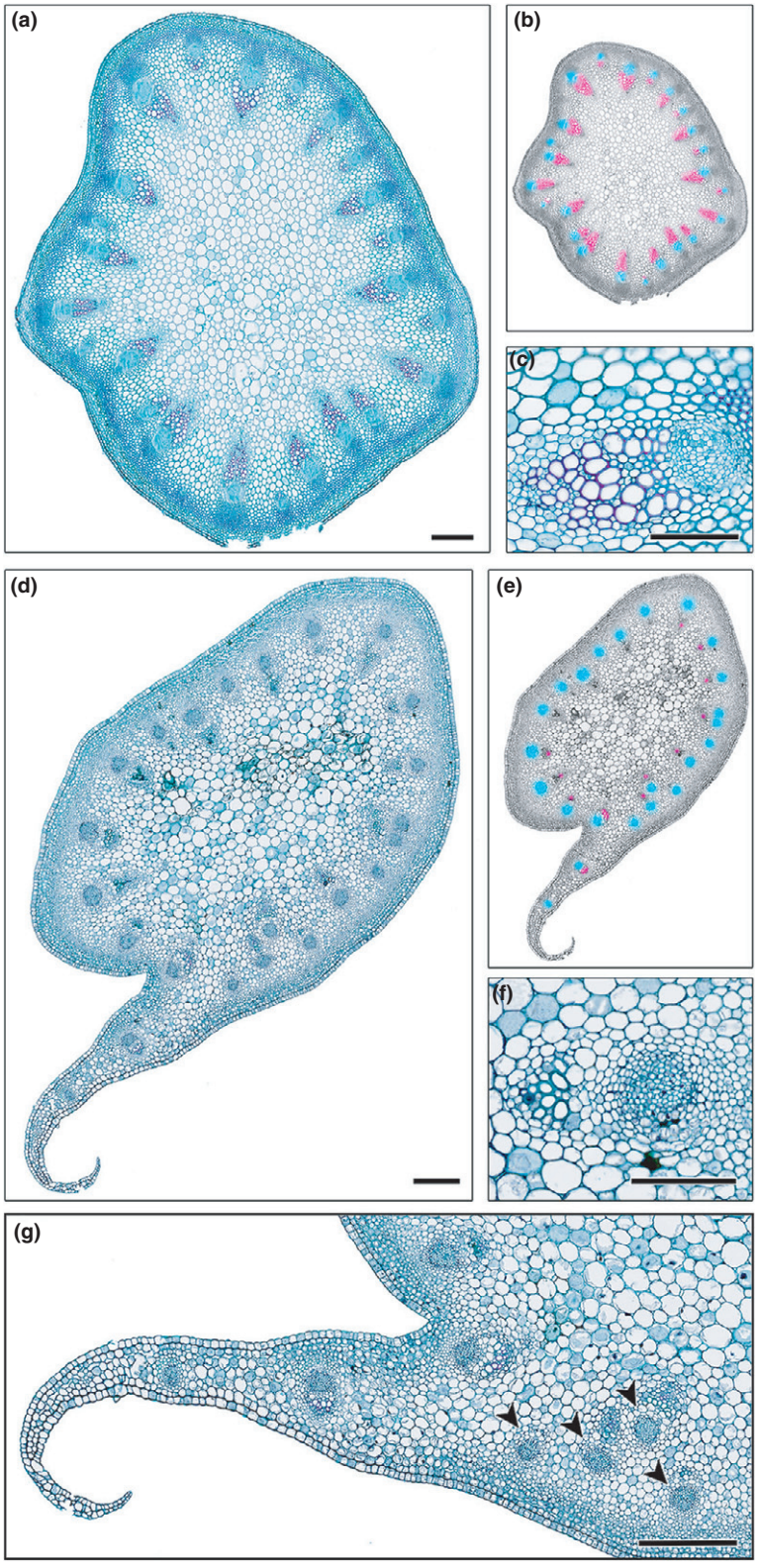

Fig. 5 Histology of (a–c) wild-type (WT) and (d–g) *AqJAG*-silenced *Aquilegia coerulea* inflorescence stems. (a) Cross section of a WT inflorescence stem. (b) False-colored overlay of (a) with xylem in magenta and phloem in blue. (c) Close-up of a WT vascular bundle. Xylem cells are on the left in the panel, discernable by pinkish staining in their lignified cell walls. (d) Cross section of an *AqJAG*-silenced inflorescence stem with outgrowth. (e) False-colored overlay of (d) with xylem in magenta and phloem in blue. (f) Close-up of a vascular bundle in *AqJAG*-silenced plants. Note the almost complete absence of lignified xylem. (g) Close-up of the outgrowth of an *AqJAG*-silenced stem. Arrowheads point at the disorganized bundles with no discernable xylem in the region adjacent to the outgrowth. Bars: (a, d, g) 200 μm; (c, f) 100 μm.

Discussion

In the present study, we investigated the developmental roles of the *Aquilegia coerulea JAGGED (AqJAG)* ortholog, allowing us to further explore its functional conservation across various taxa. Strong expression of *AqJAG* is detected in the shoot apex, floral meristem, all initiating organ primordia, and regions undergoing rapid growth, such as the developing petal spur and leaflet. Silencing of *AqJAG* led to widespread defects in both meristems and lateral organs. Leaflets are unable to expand when lacking *AqJAG* and are

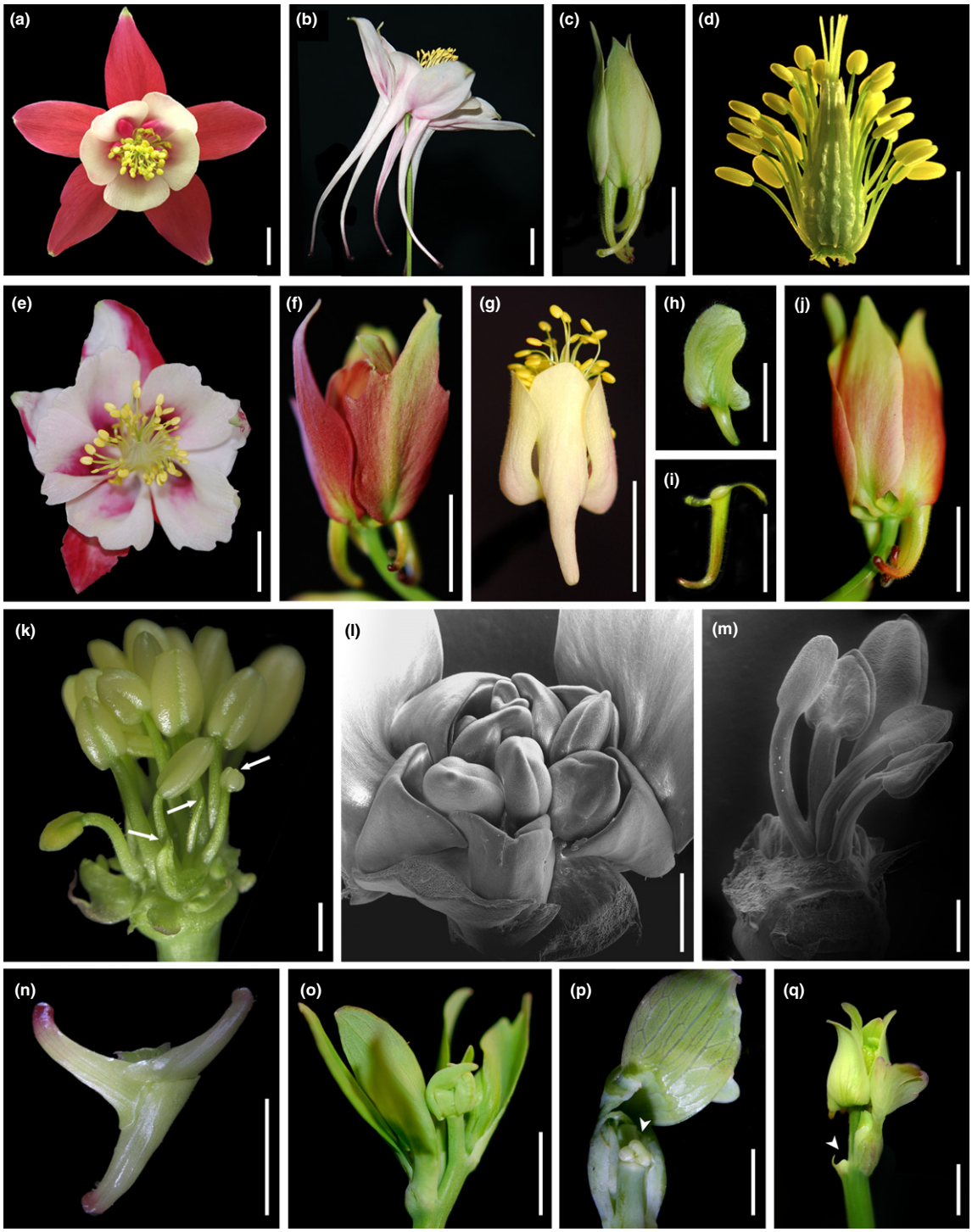

Fig. 6 Phenotypes of *AqJAG* virus-induced gene silencing (VIGS) flowers of *Aquilegia coerulea*. (a–d) Wild-type and VIGS control flowers. (a) Front view of a fully opened wild-type (WT) flower. (b) Side view of a fully opened control flower. (c) A developing pre-anthesis WT flower; during this stage, red pigmentation is just starting to appear in petals and sepals. (d) A pre-anthesis stage WT flower with perianth removed. (e–q) Phenotypes of *AqJAG*-*AqANS*-TRV2-treated flowers. (e) Flower with jagged petal margins. (f) Pre-anthesis flower with reduced sepal size, jagged sepal margins, reduced petal spur. (g) A fully opened flower with petal spurs reduced to different lengths (sepals removed). (h) Sepal–petal mosaic organ. (i) Petal–stamen mosaic organ. (j) Flower with two petals completely missing. (k) Flower with abnormal stamens (arrows) and missing carpels (perianth removed). (l) SEM of a mature flower (one sepal removed). Petal spurs failed to elongate; only few stamens developed but were abnormal; carpels were missing. (m) SEM of a mature flower (perianth removed). Only five stamens developed in the inner whorls and anthers were abnormal. (n) A mature flower having only three petals and one sepal (which was removed in the picture). (o) A terminal flower with only leaf-like organs developed. (p) A mature terminal 'flower' with no established floral organs (arrowhead). (q) An aborted axillary 'flower' (arrowhead). Bars: (a–g, j) 1 cm; (h–i, n–q) 5 mm; (k) 1 mm; (l, m) 500 μm.

concave due to changes in cell number and adaxial cell differentiation. Peculiar lamina-like outgrowths were observed on inflorescence stems, as well as reduction in the expansion of distal regions of floral organs. Some reproductive meristems terminated early or failed to produce primordia at all. Based on these results, we conclude that *AqJAG* is involved in multiple key aspects in *A. coerulea* morphogenesis, including initiation of primordia and promotion of cell proliferation and differentiation, with a disproportionate effect on the behavior of cells with adaxial identity.

AqJAG is critical to floral primordium initiation in *A. coerulea*

During the earliest stages of *A. coerulea* flower development, *AqJAG* is expressed across the floral meristem and in all initiating floral organ primordia (Fig. 2c–f). Consistent with this, many *AqJAG* VIGS flowers had missing organs, and the strongest silencing phenotypes failed to establish any floral organs at all. In less severe phenotypes, we observed mosaic floral organs, which have also been reported from the *opb* mutant in rice (Horigome *et al.*, 2009). The *opb* phenotype is considered to reflect a role as a positive regulator of the floral organ identity genes, but we do not believe that the chimeric organs in our study were due to specific interactions between *AqJAG* and the identity genes. When recovered, the combination of identities present in the mosaic organs was highly variable, as was the number of mosaic organs in each flower. We believe that this is most likely due to a mispositioning of primordia on the floral meristem, which may be caused, in turn, by differential rates of proliferation across meristems that are partially silenced for *AqJAG*. Analogous phenotypes have been observed in *shoot meristemless-2* mutants in Arabidopsis that similarly show uncoordinated proliferation in their floral meristems (Clark *et al.*, 1996).

Interestingly, these effects on meristem function seem to be more severe in the reproductive phase than the vegetative phase. Although we only recovered clearly aborted meristems in inflorescences, we recognize that it may have been too difficult to recognize a comparable phenotype in the vegetative meristem, which is completely obscured by previously produced leaves. Regardless, in all other previously examined *JAG* homologs, expression was limited to primordia themselves rather than the meristem and, in null mutants, the initiation of lateral organs seemed unaffected (Dinneny *et al.*, 2004; Ohno *et al.*, 2004; David-Schwartz *et al.*, 2009; Horigome *et al.*, 2009; Schiessl *et al.*, 2012). This suggests that the function of *AqJAG* in promoting cell proliferation may be expanded in *Aquilegia* relative to what is seen in other model systems.

AqJAG controls laminar expansion in *Aquilegia coerulea*

Consistent with earlier studies, laminar reduction is observed in *AqJAG*-silenced leaves. However, the degree of lamina reduction we recovered is on the severe end of the phenotypic spectrum when compared with the *jag*, *nub*, *lyr* or *opb* mutant phenotypes. SEM showed that the extremely stunted structures from the strongest *AqJAG*-silencing phenotypes were, in fact, established leaflet segments with distinct petioles, but laminar expansion is entirely lacking (Fig. 7a). During normal *A. coerulea* rosette leaf

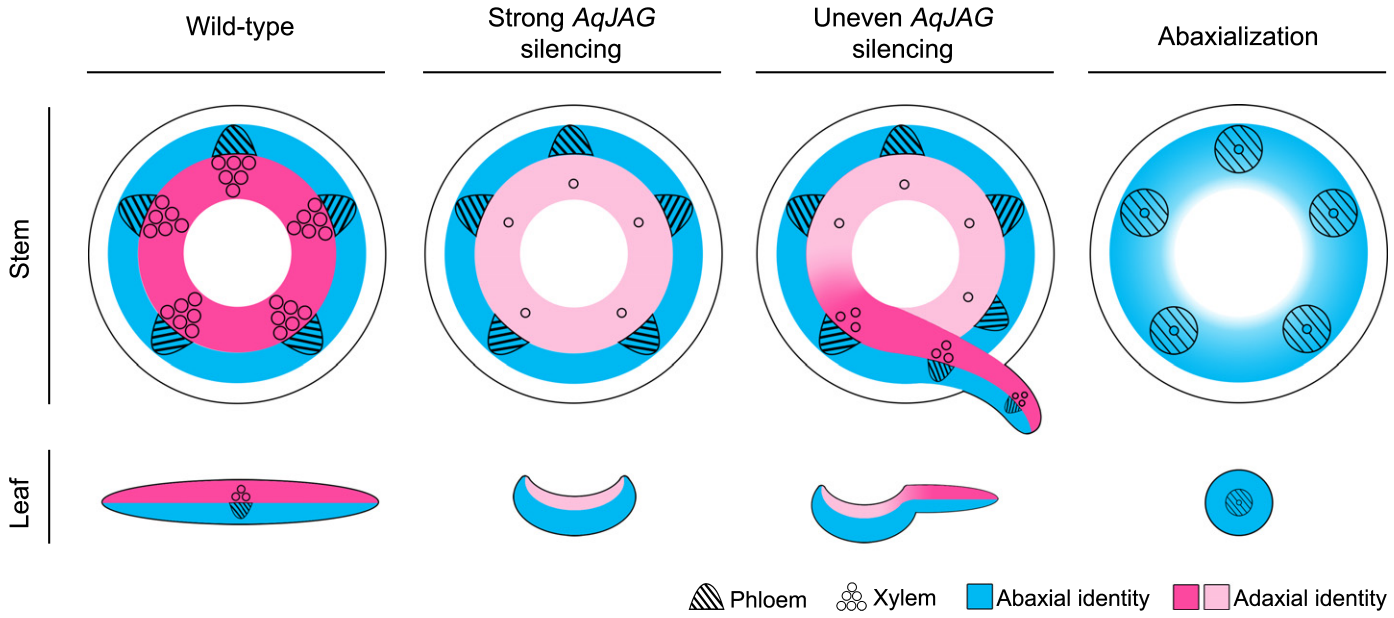

Fig. 7 Schematic that represents the relative growth of abaxial and adaxial tissues in both stems and leaves of a variety of *Aquilegia coerulea* plants. In wild-type plants, stems and leaves show clear abaxial–adaxial polarity as reflected by phloem and xylem differentiation (cross-hatching and circles, respectively), as well as differentiation of other polar cell types (blue abaxial, cells; dark pink, adaxial cells). Strong *AqJAG* silencing results in reduction in the proliferation of adaxial cell types along with improper differentiation, causing the formation of unexpanded stems and laminae. When the silencing of *AqJAG* is uneven, patches of unaffected adaxial tissue proliferate unevenly within the stem, which produces abaxial–adaxial interface zones that form ectopic laminar outgrowths along the stem. In leaves, uneven silencing result in distorted leaflets with localized patches of reduced, concave laminae. The *AqJAG* phenotypes are in distinct contrast to what is observed in true abaxialized mutants, in which vasculature and lateral organs are strongly radialized, something never observed in *AqJAG*-silenced plants.

morphogenesis, the segments of the leaflets become recognizable very soon after leaflet primordium initiation, whereas petiole elongation and the progressive expansion of laminar cells occurs much later in development (Pabón-Mora *et al.*, 2013). Within strongly silenced leaves, the most severe phenotypes are observed in lateral leaflets and lobes (Fig. 2d,h). Therefore, our observed defects are not just restricted to the distal region of growing lamina as seen in other *jag* mutants; cell proliferation in the entire leaflet lamina appears to be dramatically reduced when lacking *AqJAG*.

On the other hand, leaflet initiation itself does not appear to be dependent on *AqJAG*. Although there was no change in leaflet numbers in *AqJAG*-silenced plants, the *lyr* mutant in tomato exhibits reduced primary leaflet numbers, especially for the basal lateral pairs (David-Schwartz *et al.*, 2009). This difference could be due to a number of factors, including the fact that *Aquilegia* and tomato compound leaves are independently derived, and potential differences in the genetic programs of trifoliate vs pinnately compound leaves (Bharathan *et al.*, 2002; Harrison *et al.*, 2005). Examining *JAG* homolog functions in additional taxa bearing different types of compound leaves will be needed to determine which pattern of *JAG* function is more common.

Another difference between silencing of *JAG* in *A. coerulea* and what has been observed in other taxa is that our laminar expansion phenotypes were much more severe in vegetative organs than in floral organs. In fact, the weaker aspect of floral phenotypes for *AqJAG*-silenced flowers are much more reminiscent of *jag* or *jag nub* mutants (Dinneny *et al.*, 2004; 2006; Ohno *et al.*, 2004). Laminar expansion is primarily affected in distal regions, leading to jagged margins or failure to develop anthers. It is intriguing to see reduced nectar spur development, although not especially surprising because we have previously established that localized cell divisions are critical to formation of the spur pocket (Puzey *et al.*, 2012; Yant *et al.*, 2015). Further study will be required to understand why laminar expansion in vegetative organs of *Aquilegia* appears to be so much more dependent on *AqJAG* function than that of floral organs.

AqJAG disproportionally influences cells with adaxial identity

Perhaps the most interesting aspect of the *AqJAG*-silencing phenotype is that there is a disproportionate impact on cells with adaxial identity in both leaves and stems. Among all *AqJAG*-silenced leaflets, a concave laminar surface was always associated with lamina reduction, which appears to result from a change in both adaxial cell number and differentiation (Fig. 3). It is hard to tell at this point whether the reduction in abaxial cell number is also directly due to loss of *AqJAG* or the change is indirect and due to compensatory interactions between the two domains (Hisanaga *et al.*, 2015). Histological sectioning of affected stems revealed a substantial reduction of xylem but not phloem, which is consistent with reduced proliferation/differentiation of adaxial cell types (Emery *et al.*, 2003). However, these vascular bundles are collateral rather than amphicribral, suggesting that the tissue is not truly abaxialized (Waites & Hudson, 1995). We, therefore, conclude that *AqJAG* differentially influences the behavior of adaxial cells rather than determining their identity; without its proper expression, adaxial cells fail to proliferate and differentiate in the vegetative tissues of *A. coerulea*.

The lamina-like outgrowth in *AqJAG*-silenced inflorescence axes is a rather peculiar phenotype, and to our knowledge, similar defects in stems have not been characterized previously in any *JAG* homolog mutants. We propose the following model to explain the phenomenon (Fig. 7). Wild-type stems are radially patterned with adaxial identity positioned internally and abaxial positioned externally. When the stem experiences broad and strong silencing of *AqJAG*, we would predict that vascular bundles remain collateral but with severely under-proliferated adaxial cells, including the xylem. However, due to the nature of VIGS, silencing is often patchy or temporally variable, which can lead to unsilenced or weakly silenced patches in the stem where adaxial cells undergo relatively normal proliferation. The interaction between this kind of patch of adaxial identity and the surrounding abaxial tissue appears to create a margin that leads to laminar outgrowth, similar to what is normally seen in lateral organs (Waites & Hudson, 1995).

Although no previous study of *JAG* homologs has shown adaxial-specific defects as severe as ours, the phenotypes we obtained are not entirely surprising. Several lines of evidence suggest the involvement of *JAG* in polarity-related pathways and raise the possibility of an ancestral role for *JAG* homologs in adaxial cell development. For instance, both *LYR* from tomato and *NUB* from Arabidopsis show adaxial-specific expression in lateral organs, with the *NUB* expression being consistently adaxial across many organ types (David-Schwartz *et al.*, 2009; Dinney *et al.*, 2006). Although *lyr* mutants do not have dramatic adaxial defects, there is some loss or reduction of adaxial cell types combined with expansion of abaxial cell types. Ectopic expression of *NUB* promotes development of trichomes on the abaxial surface of leaves and the double *nub jag* mutant exhibits reproductive organ phenotypes that appear to be due to underproliferation/-differentiation of cells with adaxial identity (Dinney *et al.*, 2006). The authors of that study hypothesized that *JAG* and *NUB* may promote the competence of tissues to response to the polarity pathways, a theory that is consistent with our results. It is also interesting to consider the connections between *JAG*, organ polarity, and the *BOP* genes. The *bop1-1* mutant in Arabidopsis displays laminar outgrowths on the petiole, somewhat analogous to our stem outgrowths (Ha *et al.*, 2003). *BOP*s are known to antagonistically interact with *JAG* but also to differentially regulate the expression of adaxial determinants *PHABULOSA* and *PHAVOLUTA* and abaxial determinants *KAN1* (Norberg *et al.*, 2005; Ha *et al.*, 2007). Further studies are necessary to understand the potential interactions between *JAG/NUB* and other polarity determinants in the major model systems, as well as *A. coerulea*.

Although researchers have achieved a fairly sophisticated understanding of how the interaction of adaxial–abaxial identity promotes lateral organ growth, we are still in the early stages of determining how these identities are fully realized in terms of

cell proliferation and development. Even when we consider a simple flat leaf, we observe complex differential regulation of cell growth and cell types in each domain. Our current results, therefore, provide evidence that cell proliferation could be controlled in an identity-specific manner such that adaxial cell division acts primarily through *JAG* homologs whereas abaxial cells rely on other pathways. Interestingly, this dependence on *AqJAG* in *Aquilegia* for laminar expansion may be more pronounced in vegetative organs than reproductive. Given that there are several genetic pathways to control cell proliferation (Doonan, 2000; Gutierrez, 2005; Hepworth & Lenhard, 2014) as well as adaxial identity (Fukushima & Hasebe, 2014), it is perhaps not surprising to find that over the course of evolutionary time, developmental system drift has led to different patterns of redundancy and functional dominance among these different genetic modules.

Acknowledgements

The authors would like to thank members of the Kramer lab, Evangeline Ballerini, and three anonymous reviewers for helpful comments on the manuscript. This work was supported by NSF award IOS-1121005 to E.M.K.

Author contributions

The study was conceived of and designed by Y.M. and E.M.K. All experiments and data collection were conducted by Y.M. with training and oversight provided by E.M.K. The manuscript was written and figures prepared by Y.M. with revisions by E.M.K.

References

Altschul SF, Gish W, Miller W, Myers EW, Lipman DJ. 1990. Basic local alignment search tool. *Journal of Molecular Biology* **215**: 403–410.

Bharathan G, Goliber TE, Moore C, Kessler S, Pham T, Sinha NR. 2002. Homologies in leaf form inferred from KNOXI gene expression during development. *Science* **296**: 1858–1860.

Ciftci-Yilmaz S, Mittler R. 2008. The zinc finger network of plants. *Cellular and Molecular Life Sciences* **65**: 1150–1160.

Clark SE, Jacobsen SE, Levin JZ, Meyerowitz EM. 1996. The *CLAVATA* and *SHOOT MERISTEMLESS* loci competitively regulate meristem activity in *Arabidopsis*. *Development* **122**: 1567–1575.

Dale JE. 1988. The control of leaf expansion. *Annual Review of Plant Physiology and Plant Molecular Biology* **39**: 267–295.

David-Schwartz R, Koenig D, Sinha NR. 2009. *LYRATE* is a key regulator of leaflet initiation and lamina outgrowth in tomato. *Plant Cell* **21**: 3093–3104.

Dinneny JR, Weigel D, Yanofsky MF. 2006. NUBBIN and JAGGED define stamen and carpel shape in *Arabidopsis*. *Development* **133**: 1645–1655.

Dinneny JR, Yadegari R, Fischer RL, Yanofsky MF, Weigel D. 2004. The role of *JAGGED* in shaping lateral organs. *Development* **131**: 1101–1110.

Doonan J. 2000. Social controls on cell proliferation in plants. *Current Opinion in Plant Biology* **3**: 482–487.

Emery JF, Floyd SK, Alvarez J, Eshed Y, Hawker NP, Izhaki A, Baum SF, Bowman JL. 2003. Radial patterning of *Arabidopsis* shoots by Class III HD-ZIP and KANADI genes. *Current Biology* **13**: 1768–1774.

Englbrecht CC, Schoof H, Böhm S. 2004. Conservation, diversification and expansion of C2H2 zinc finger proteins in the *Arabidopsis thaliana* genome. *BMC Genomics* **5**: 39.

Eshed Y, Izhaki A, Baum SF, Floyd SK, Bowman JL. 2004. Asymmetric leaf development and blade expansion in *Arabidopsis* are mediated by KANADI and YABBY activities. *Development* **131**: 2997–3006.

Fukushima K, Hasebe M. 2014. Adaxial–abaxial polarity: the developmental basis of leaf shape diversity. *Genesis* **52**: 1–18.

Fukushima K, Fujita H, Yamaguchi T, Kawaguchi M, Tsukaya H, Hasebe M. 2015. Oriented cell division shapes carnivorous pitcher leaves of *Sarracenia purpurea*. *Nature Communications* **6**: doi: 10.1038/ncomms7450.

Gould B, Kramer EM. 2007. Virus-induced gene silencing as a tool for functional analyses in the emerging model plant *Aquilegia* (columbine, Ranunculaceae). *Plant Methods* **3**: 6.

Gutierrez C. 2005. Coupling cell proliferation and development in plants. *Nature Cell Biology* **7**: 535–541.

Ha CM, Jun JH, Nam HG, Fletcher JC. 2007. *BLADE-ON-PETIOLE1* and *2* control *Arabidopsis* lateral organ fate through regulation of LOB domain and adaxial–abaxial polarity genes. *Plant Cell* **19**: 1809–1825.

Ha CM, Kim GT, Kim BC, Jun JH, Soh MS, Ueno Y, Machida Y, Tsukaya H, Nam HG. 2003. The *BLADE-ON-PETIOLE1* gene controls leaf pattern formation through the modulation of meristematic activity in *Arabidopsis*. *Development* **130**: 161–172.

Harrison CJ, Corley SB, Moylan EC, Alexander DL, Scotland RW, Langdale JA. 2005. Independent recruitment of a conserved developmental mechanism during leaf evolution. *Nature* **434**: 509–514.

Hepworth J, Lenhard M. 2014. Regulation of plant lateral-organ growth by modulating cell number and size. *Current Opinion in Plant Biology* **17**: 36–42.

Hisanaga T, Kawade K, Tsukaya H. 2015. Compensation: a key to clarifying the organ-level regulation of lateral organ size in plants. *Journal of Experimental Botany* **66**: 1055–1063.

Horigome A, Nagasawa N, Ikeda K, Ito M, Itoh J-I, Nagato Y. 2009. Rice *OPEN BEAK* is a negative regulator of class I *knox* genes and a positive regulator of class B floral homeotic gene. *Plant Journal* **58**: 724–736.

Jones DT, Taylor WR, Thornton JM. 1992. The rapid generation of mutation data matrices from protein sequences. *CABIOS* **8**: 275–282.

Jun JH, Ha CM, Fletcher JC. 2010. *BLADE-ON-PETIOLE1* coordinates organ determinacy and axial polarity in *Arabidopsis* by directly activating *ASYMMETRIC LEAVES2*. *Plant Cell* **22**: 62–76.

Kramer EM. 2005. Methods for studying the evolution of plant reproductive structures: comparative gene expression techniques. *Methods in Enzymology* **395**: 617–636.

Kramer EM, Hodges SA. 2010. *Aquilegia* as a model system for the evolution and ecology of petals. *Philosophical Transactions of the Royal Society of London. Series B: Biological Sciences* **365**: 477–490.

Larkin MA, Blackshields G, Brown NP, Chenna R, McGettigan PA, McWilliam H, Valentin F, Wallace IM, Wilm A, Lopez R, *et al.* 2007. Clustal W and Clustal X version 2.0. *Bioinformatics* **23**: 2947–2948.

Livak KJ, Schmittgen TD. 2001. Analysis of relative gene expression data using real-time quantitative PCR and the $2^{-\Delta\Delta CT}$ method. *Methods* **25**: 402–408.

Nakata M, Matsumoto N, Tsugeki R, Rikirsch E, Laux T, Okada K. 2012. Roles of the middle domain-specific *WUSCHEL-RELATED HOMEOBOX* genes in early development of leaves in *Arabidopsis*. *Plant Cell* **24**: 519–535.

Norberg M, Holmlund M, Nilsson O. 2005. The *BLADE ON PETIOLE* genes act redundantly to control the growth and development of lateral organs. *Development* **132**: 2203–2213.

Ohno CK, Reddy GV, Heisler MGB, Meyerowitz EM. 2004. The *Arabidopsis JAGGED* gene encodes a zinc finger protein that promotes leaf tissue development. *Development* **31**: 1111–1122.

Pabón-Mora N, Sharma B, Holappa LD, Kramer EM, Litt A. 2013. The *Aquilegia FRUITFULL*-like genes play key roles in leaf morphogenesis and inflorescence development. *Plant Journal* **74**: 197–212.

Pekker I, Alvarez J, Eshed Y. 2005. Auxin response factors mediate *Arabidopsis* organ asymmetry via modulation of KANADI activity. *Plant Cell* **17**: 2899–2910.

Puzey JR, Gerbode SJ, Hodges SA, Kramer EM, Mahadevan L. 2012. Evolution of spur-length diversity in *Aquilegia* petals is achieved solely through cell-shape anisotropy. *Proceedings of the Royal Society B: Biological Sciences* **279**: 1640–1645.

Ruzin ES. 1999. *Plant microtechnique and microscopy, vol. 198*. New York, NY, USA: Oxford University Press.

Sarojam R, Sappl PG, Goldshmidt A, Efroni I, Floyd SK, Eshed Y, Bowman JL. 2010. Differentiating Arabidopsis shoots from leaves by combined YABBY activities. *Plant Cell* **22**: 2113–2130.

Schiessl K, Kausika S, Southam P, Bush M, Sablowski R. 2012. *JAGGED* controls growth anisotropy and coordination between cell size and cell cycle during plant organogenesis. *Current Biology* **22**: 1739–1746.

Sharma B, Guo C, Kong H, Kramer EM. 2011. Petal-specific subfunctionalization of an *APETALA3* paralog in the Ranunculales and its implications for petal evolution. *New Phytologist* **191**: 870–883.

Sharma B, Kramer EM. 2013a. Virus-induced gene silencing. *Methods in Molecular Biology* **975**: 71–81.

Sharma B, Kramer EM. 2013b. Sub- and neofunctionalization of *APETALA3* paralogs have contributed to the evolution of novel floral organ identity in *Aquilegia* (columbine, Ranunculaceae). *New Phytologist* **197**: 949–957.

Siegfried KR, Eshed Y, Baum SF, Otsuga D, Drews GN, Bowman JL. 1999. Members of the *YABBY* gene family specify abaxial cell fate in *Arabidopsis*. *Development* **126**: 4117–4128.

Stamatakis A, Hoover P, Rougemont J. 2008. A rapid bootstrap algorithm for the RAXML Web servers. *Systematic Biology* **57**: 758–771.

Toriba T, Suzaki T, Yamaguchi T, Ohmori Y, Tsukaya H, Hirano HY. 2010. Distinct regulation of adaxial–abaxial polarity in anther patterning in rice. *Plant Cell* **22**: 1452–1462.

Vandenbussche M, Horstman A, Zethof J, Koes R, Rijpkema AS, Gerats T. 2009. Differential recruitment of *WOX* transcription factors for lateral development and organ fusion in Petunia and *Arabidopsis*. *Plant Cell* **21**: 2269–2283.

Waites R, Hudson A. 1995. *phantastica*: a gene required for dorsoventrality of leaves in *Antirrhinum majus*. *Development* **121**: 2143–2154.

Yant L, Collani S, Puzey J, Levy C, Kramer EM. 2015. Molecular basis for three-dimensional elaboration of the *Aquilegia* petal spur. *Proceedings of the Royal Society B: Biological Sciences* **282**: 20142778.

Supporting Information

Additional Supporting Information may be found online in the Supporting Information tab for this article:

Fig. S1 Predicted amino acid alignment of AqJAG, AtJAG, AtNUB, AtSUP and OsOPB.

Fig. S2 Maximum likelihood tree showing the relationships among amino acid sequences encoded by 42 AtJAG homologs and 14 Arabidopsis C2H2 zinc-finger proteins.

Fig. S3 Quantitative RT-PCR showing the downregulation of *AqJAG*.

Table S1 Stages of *Aquilegia* floral development.

Please note: Wiley Blackwell are not responsible for the content or functionality of any Supporting Information supplied by the authors. Any queries (other than missing material) should be directed to the *New Phytologist* Central Office.